NJC

Accepted Manuscript

This article can be cited before page numbers have been issued, to do this please use: L. Li, X. Wang, Z. Li, Y. Li, Y. Qi and Q. Dong, *New J. Chem.*, 2015, DOI: 10.1039/C5NJ01772F.

ROYAL SOCIETY OF CHEMISTRY

www.rsc.org/njc

View Article Online
DOI: 10.1039/C5NJ01772F

Journal Name

RSCPublishing

ARTICLE

The synthesis and curing kinetics study of a new fluorinated polyurethane with fluorinated side chains attached to soft blocks

Cite this: DOI: 10.1039/x0xx00000x

Lingling Li [a,b],Xia Wang [b*],Zan Li [c] , Ying Li [b*], Yuanchun Qi [a], Qingzhi Dong [a*]

Received ooth January 2012,
Accepted ooth January 2012

DOI: 10.1039/x0xx00000x

www.rsc.org/

Fluorinated polyurethane (FPU) with fluorine in the side chain was obtained using fluorinated polyether glycol (FPO) with fluorinated side chains and 4,4'-diphenyl methane diisocyanate (MDI). The direct visual inspection of microstructures by SEM revealed that the separation degree of soft and hard segments decreased as the introduction of fluorinated groups into polyurethanes soft segments, leading to a decrease in the crystallinity of FPU. The glass transition temperatures (T_g) measured by DMA indicated that the optimal working temperature window of FPU separating soft and hard glass transitions became narrow. And the mechanical properties and surface properties of the FPU were also measured.Curing kinetics of FPU was studied by rotational rheometer, and the activation energy of FPU was obtained. The relationship between the curing temperature and mobility of fluorinated groups was characterized by XPS. The result showed that F content in the FPU surface decreased with increasing curing temperature.

Introduction

Polyurethanes (PUs) are used in a wide variety of applications, such as protective coatings, elastomers, sealants, adhesives, and foams.[1-6]Also, fluorinated polyurethanes (FPUs), which incorporate fluorinated blocks into the molecular chains, not only maintain most of the outstanding properties of PUs, but also offer many useful and desirable features, such as unique surface properties, high thermal stability and chemical resistance. [7-10]

Fluorocarbon chains have been incorporated into polyurethanes by fluorinated diisocyanates, chain extenders, polyether glycols, polyester glycols and end-cappers. [11-17]However, because of the higher syntheticcost, fewer varieties of fluorinated diisocyanates, and lower molecular weight of fluorinated alcohols, the improvement of properties of fluorinated polyurethane prepared was not significant compared with hydrogenatedpolyurethane.[8,18]Now, most FPUs are synthesized by fluorinated polyether glycols as soft segments. Yoon S.C, et al.[19,20]proposed that the soft segments have higher mobility and easily migrate to the surface region at room temperature. P. F. Liu, et al.[21]synthesized FPUs with fluoropolydiol. Owing to the high amount of fluorinated blocks in the main-chain of the polymer, FPUs have excellent mechanical properties, low surface tension and high temperature performance. M. Castellano, et al.[22] synthesized a series of fluorinated polyurethanes using perfluoropolyether (PFPE) and poly-ε-caprolactone (PCL) as soft blocks via different polymerization procedure. They found that the strong incompatibility between hydrogenated and fluorinated components and between low-polar soft segments (PCL) and polar hard blocks was an effective driving force promoting the microphase segregation. And polymerization procedure was a key parameter for ruling the composition of polymeric chains, but it had little effect on the surface properties. Tao Liu, et al.[23]synthesized fluorinated polyurethane fluorine-containing pendent groups in soft segments using polybutyleneadipate (PBA) to be compounded with fluorinate polyether diol (PFGE) as the soft-segment of FTPU. Fluorine can be enriched on the surface during processing resulting in the high content of fluorine on the surface, and the surface tension significantly decreased. R. P. Jia, et al.[24]used polyetherpolyol containing fluorine in the side chain and polytetramethylene ether glycol (PTMEG) as soft segment to obtain fluorinated polyurethane, However, the properties of fluorinated polyurethanes were strongly dependent on the mass ratio and segment compatibility of the mixed soft-segment.

A number of studies have been carried out on the structure, morphology, and properties of FPUs. Nevertheless, only a few studies have been published on the curing kinetics of FPUs. Owing to the low polarizability and strong electronegativity of the fluorine atom, the reactivity of hydroxy-terminated

View Article Online
DOI: 10.1039/C5NJ01772F
Journal Name

fluorinated polyether glycols is surely different from the conventional polyether diols [25,26]. Leonid，et al.[27]studied the urethane reactions of cycloaliphatic and aromatic diisocyanates with hydroxyl-terminated fluoropolyethers (FPEs). They proposed that the FPEs diols were attributed to the autocatalysis of isocyanate-hydroxyl reaction, and also, the reactivity with diisocyanates strongly depended on the structure of FPEs and their molecular weights. S. Turri et al.[28]studied the catalyst effect on the crosslinking kinetics of fluorinated polyurethane**.** The aim of this investigation was to elucidate thecuring kinetics of FPU and the relationship between the curing temperature and mobility of fluorinated groups. In order to carry it out, firstly, we prepared fluorinated polyether glycol with fluorine-containing side chains (FPO) via "living/controlled" cationic ring-open polymerization of tetrahydrofuran (THF) and fluorine-containing epoxy compounds (FO). Then FPU with fluorine-containing pendent groups in soft segments was obtained using FPO as soft segment. The morphology, dynamics, crystallization, thermal properties and Surface properties of FPU were investigated. Last but not least, curing kinetics of FPU was studied by the rotational rheometer. And the effect of curing temperature on mobility of fluorinated groups was studied by X-ray Photoelectron Spectroscopy(XPS).

Experimental

Materials

Diphenyl-methane-diisocyanate (MDI, Sigma, USA), and 1,4-Butanediol (BDO, AR, Shanghai, China) were distilled under vacuum and dried over 4 Å molecular sieves. THF (AR, Shanghai, China) was kept for 48 h over KOH pellets to remove peroxide. After filtration, the THF was heated over sodium for 12 h and then distilled. Ethylene glycol (EG) was distilled twice. Methylene chloride (AR, Shanghai, China) was washed three times with concentrated sulfuric acid to remove unsaturated impurities and then washed several times with water, a 5% solution of $NaHCO_3$, and again with distilled water. After drying for 24 h over $CaCl_2$, the methylene chloride was distilled over CaH_2 and kept in a vacuum ampoule over fresh CaH_2. The 2,2,3,3-tetrafluoro-1-propanol (TFP, Sigma, USA),1-propyl alcohol (1-PA) and epichlorohydrin (ECH) (AR, Shanghai, China) were used as supplied. Initiator $BF_3{\cdot}OEt_2$ (AR, Shanghai, China) was used after purified by vacuum distillation.

Synthesis of fluorinated polyether glycols and hydrogenated polyether glycols

Stoichiometric amounts of the ECH and cyclohexane (as water-carrying agent) were charged into the 3-necked round bottom flask equipped with a mechanical stirrer under a dry nitrogen atmosphere. When the temperature was raised to 80 °C, NaOH and TFP were fed dropwise in 2 h. The reaction mixture was kept for another 3 h at 80 °C. Fluorinated epoxy compound (FO) was obtained after purified by vacuum distillation.[29] Fluorinated polyether glycol (FPO) was prepared by slowly adding FO to the reaction mixture containing bulk THF, EG and $BF_3{\cdot}OEt_2$ under nitrogen at 0 °C in a glass flask and kept for 5 h. Then FPO was obtained after washing and distillation.[30] Hydrogenated polyether glycol (HPO) was also prepared, the synthesized process and reaction conditions of HPO were almost the same as these of the fluorinated polyether glycol, except using 1-PA instead of TFP.

Synthesis of fluorinated polyurethane and hydrogenated polyurethane

The fluorinate polyurethane (FPU) was synthesized using FPO as soft segments, MDI as hard segments and BDO as a chain extender. Under nitrogen atmosphere at 50 °C, the stoichiometric amount of MDI was added into a four-necked flask equipped with a heating mantle, a mechanical stirrer, and a thermometer. After dissolution，FPO was added dropwise into four-necked flask. The temperature was raised to 80 °C and kept for 3 h. Then the temperature was reduced to 40 °C. The stoichiometric amount of chain extender was added dropwise. Finally the polymers were dried in vacuum at70 °C for 16 h. The reaction completion was monitored by the absence of IR- free NCO group at 2270 cm^{-1}. The whole reaction processes are depicted in Scheme 1. Hydrogenated polyurethane (HPU) was also obtained for comparison purpose. The synthetic process and reaction conditions were the same as these of fluorinated polyurethanes, except using HPO as the soft segment.The material composition and molecular weights were listed in table 1.

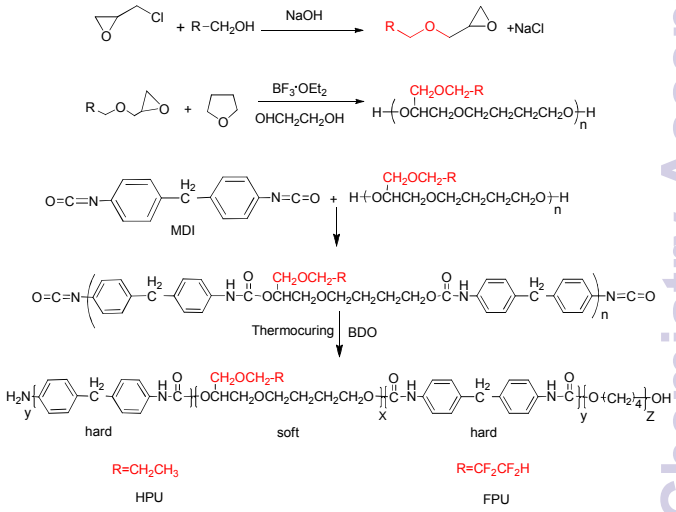

Scheme 1. The reaction process of FPU and HPU

Journal Name View Article Online DOI: 10.1039/C5NJ01772F ARTICLE

Table1 The material composition and molecular weights

Material	Molar ration HPO(FPO)/MDI/BDO	Soft segments(Mn) (g/mol)	Hard segment Wt.-%	$\overline{M}_n \times 10^4{}_{GPC}$ (g/mol)	MWD_{GPC}
HPU	1/3/2	HPO-650	53.6	2.16	3.17
FPU	1/3/2	FPU-670	47.2	2.70	3.10

Measurements

FTIR analysis

The composition of the synthesized FPU was analyzed with Fourier-transform infrared spectrometer (FTIR) spectra (Perkin Elmer, SPECTRUM 100). The specimen was prepared by casting the polymer solution film on KBr discs. 32 scans were averaged for each sample in the range of 4000-400 cm^{-1} at resolution of 4 cm^{-1}.

^{1}H NMR and ^{19}F measurements

^{1}H NMR and ^{19}F NMR was recorded on a Bruker AC 400 NMR spectrometer with tetramethylsilane (TMS) as internal standard and deuterated dimethyl sulphoxide (DMSO-d_6) as solvent.

GPC analysis

The molecular weights of HPU and FPU were characterized using PL-GPC50 Gel-Permeation Chromatograph (GPC) with DMF as eluent at a flow rate of 1.0 ml/min. The measurement was carried out at 50 ^oC.

SEM analysis

The fracture morphologies of FPU and HPU were assessed using S-4800 field emission scanning electron microscope (FESEM; Hitachi, Japan). Samples were treated under liquid nitrogen before observation.

Thermal Characterization

The thermal response of HPU and FPU was characterized using a PE 8500 differential scanning calorimeter. The response was measured over a temperature range of -50 to250 ^oC at a heating and cooling rate of 10 K/min under a nitrogen flow of 50 mL/min.

Dynamic mechanical analysis (DMA)

Dynamic mechanical properties were measured on a dynamic mechanical thermal analyzer (NETZSCH, DMA 242). All the samples were measured with compression mode at a heating rate of3K/min, DF/CSF is 3.00N/0.30N. at a frequency of 1 Hz over a temperature range -80−200 ^oC. The sample size was 1.6×5.6×7.8mm^3.

X-ray diffractograms analysis (XRD)

X-ray diffractograms analysis was performed on a D8 Advance apparatus (Bruker, Germany) in the range of 2θ = 5-40^o, with a nickel-filtered Cu K-radiation (k = 0.154 nm) at an operation voltage of 40 kV and 30 mA, scan rate is 5^o/min.

The thermal stabilities analysis

The thermal stabilities FPU and HPU were carried out using a Perkin Elmer（PE）Pyris TGA thermo gravimetric analyzer from room temperature to 800 ^oC at 10 K/min heating rates with N_2 protection, the weights of sample are 3-8 mg in all cases.

Tensile properties analysis

The tensile properties of FPU and HPU were measured using a Materials Testing Machine at room temperature and relative humidity of 50%. A cross-head speed of 10mm/min was used to determine the ultimate tensile strength and modulus as well as the elongation at break. The results reported are the mean values for five replicates.

Surface properties analysis

The surfaces properties of the HPU and FPU were analyzed by XPS and contact angles. XPS (PHI 5000 Versa Probe, Japan)was equipped with monochromated AlKa X-ray source (15 kV, 25 W) and take-off angle of 45^{o}was used with X-ray source.

The contact angles (DSA 30 KRUSS, Germany) were measured by the sessile drop method using telescoping goniometers at room temperature. 5-10 μL distilled water was pumped from a microsyringe onto the surfaces of the HPU and FPU film, the image was captured using a telescope fitted with a video camera. All the results were expressed as the average value of at least five independent measurements.

Curing kinetics analysis

The curing kinetics of HPUs and FPUs were performed in an Haake Mars-ⅢIrotational rheometer (Thermo Scientific, Germany) with a cone-plate geometry (diameter of 20 mm, gap of 0.5 mm).Oscillatory measurement was oscillatory time sweep, t=15min. The oscillation frequency was 1Hz.

View Article Online
DOI: 10.1039/C5NJ01772F
Journal Name

Results and discussion

FPU structure characterization

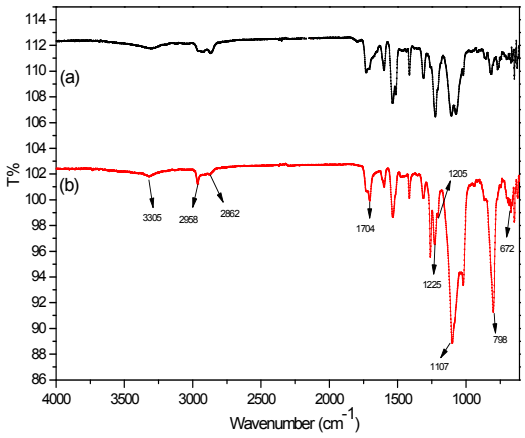

Fig. 1 FTIR spectra of (a) HPU (b) FPU**.**

The FTIR spectrums of HPU (a) and FPU (b) are show in Fig. 1. In the spectrum, there are characteristic peaks of N-H (3305 cm^{-1}). The characteristic bands at 1704cm^{-1}, 1107cm^{-1} confirm the carbonyl group of urethane, ether (C-O-C) of the ester group. There are C-H aliphatic stretches bands at 2958，2862cm^{-1}. Compared with Fig.1 (a), the absorption bands dealing with the vibration absorption of C-F bond are observed from Fig.1 (b).The stronger characteristic absorption bands locating at 1225，1205 cm^{-1} can be attributed to stretching vibrations of -CF_2.[31,32]And a combination of rocking and wagging vibration of CF_2 group at 798，672 cm^{-1} in the fingerprint region is detected. It can be concluded that F has been introduced into polyurethane. In addition, the absorption bands of the NCO group (2270 cm^{-1})and the OH group (3340 cm^{-1}) are not found in the spectrum.

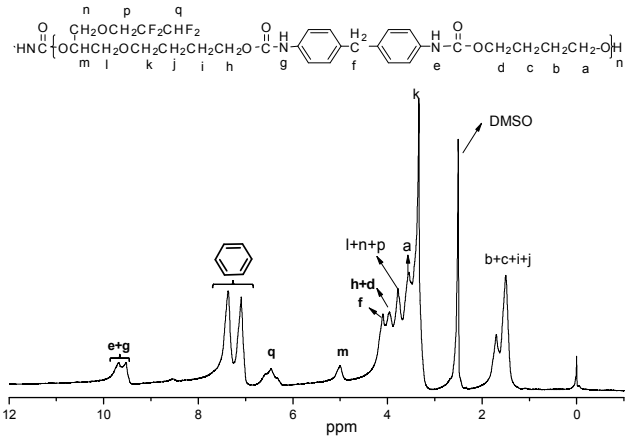

Fig. 2 ^{1}H NMR spectrum of FPU.

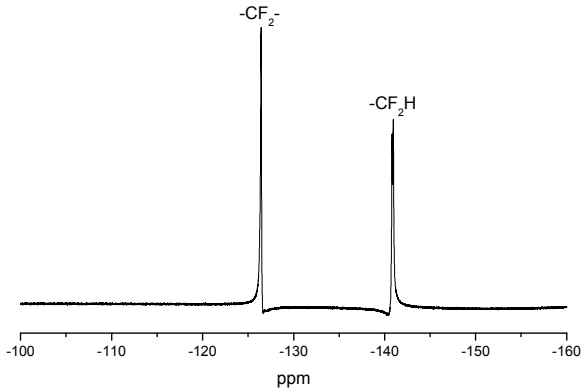

Fig. 3 ^{19}F NMR spectrum of FPU.

The ^{1}H NMR spectrum of FPU is shown in Fig. 2. It is evident that the peak appears at 9.5 ppm, which is assigned to the protons of -OCON**H**-. The peaks at 6.33-6.25 ppm are relative to the fluoromethenyl protons (-C**H**F_2), the peaks at 1.51-1.69 ppm assigned to the -$OCH_2C\mathbf{H_2}C\mathbf{H_2}CH_2O$- protons of BDO, THF. The peaks at 3.68-3.88ppmdealing with –$O\mathbf{H_2}CCH(O)$-$C\mathbf{H_2}O$-, -$OC\mathbf{H_2}CF_2$ protons and the peaks assigned to the -OC**H**- protons (5.0 ppm) are also observed in the ^{1}H NMR spectrum of FPU. The peak at 3.95 ppm is assigned to the protons of –$COOC\mathbf{H_2}$-. The peak appears at 7.37-7.09 ppm is assigned to the protons of phenyl. And[19] F NMR (Fig.3) for FPU shows two different peaks remarkably. The resonant absorbance of fluorine in-C**F**$_2$- group shifted to -126.4 ppm. The resonance of the fluorine in -CF_2H is observed at about -140.8 ppm. The results of ^{1}H NMR and ^{19}F NMR indicate that FPU based MDI and FPO has been prepared successfully.

Microstructures of HPU and FPU

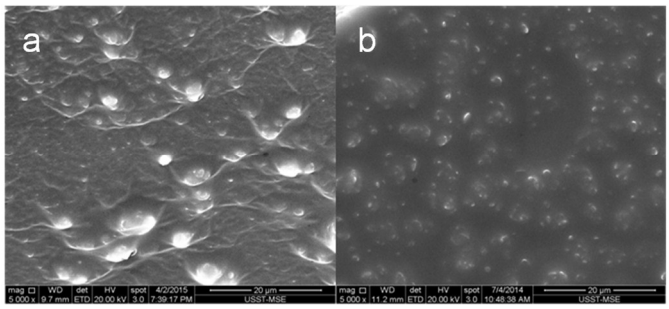

Fig.4 SEM fracture surface of (a) HPU and (b) FPU

In this study,SEM was used to understandthe bulk morphology of fluorinated polyurethane. Fig.4. displayed the SEM images of fractured surfaces ofHPU and FPU. All samples exhibit typical microphase separation morphology with dispersed hard domains in a continuous soft phase as is reported.[33]It can be seen that the image of the HPU displays numerous micron-sized particles on the fracture surfaces. When F was introduced into soft segment, the size of particles decreased, meanwhile the intermediate phase interface became smoother, indicating that the compatibilityofthe fluorinated soft and the hard segments was enhanced. This is because that fluorine with strong electro easily form hydrogen bond with N-H of the urethanes groups, leading to the enhancement of interactions

Journal Name

View Article Online
DOI: 10.1039/C5NJ01772F

between soft and hard semgent , and decrease of degree of microphase separation.[34]It is believed that the introduction of polar group into the side chains has an influence on the formation of H-bond within PU, thereby affecting the microphase separation.[35]

XRD analysis

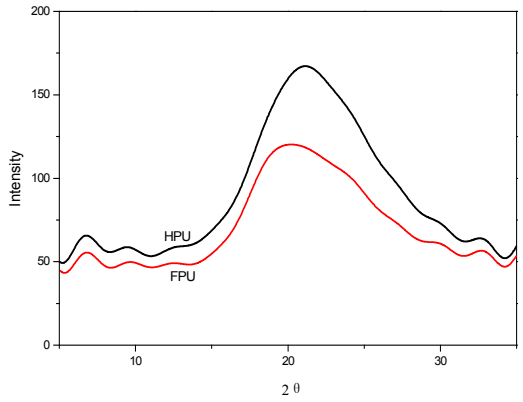

Fig.5 XRD patterns of HPU and FPU

Fig.5. shows the XRD patterns of HPU and FPU samples at room temperature. The feature at 21 ° as diffraction peaks observed for polyurethanes arising from crystallinity in the hard domains[36]. It can be found that 2θ at 21 ° becomes decreasingly evident for FPU, suggesting that the introduction of F into soft segments decreases the level of the degree of crystallinity in the polyurethane. However, they are much subtler than the diffraction patterns, indicating very low degree of hard segment crystallinity arising from ordered urea linkages.

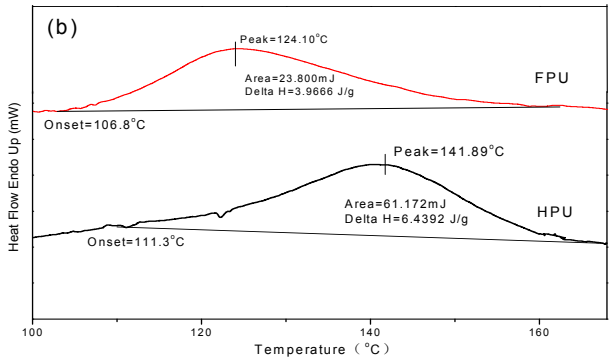

Fig.6 DSC thermogrames of HPU and FPU(a)DSC curve,(b) the magnified graph of endothermic peaks at higher temperature.

The DSC heating curves of HPU and FPU are shown in Fig. 6(a). the Fig.6 (b) showed the magnified graph of endothermic peaks. The enthalpy □H was determined by integration of the peak areas. The T_g and other thermal characteristics results are summarized in Table 2.It can be seen that T_g of soft segment is observed in each sample. At higher temperatures, the existence of minor endothermic peaks results from the dissociation of domains containing long-rang order. [37]And the melting peak relatively decreases after introducing fluorine on the soft segments. This result indicates that in FPU the association of domains with long-range order becomes much lower. In the cooling scans (dotted lines in Fig6), no exothermic peak is observed in any of the materials, indicting the low degree of hard segment crystallinity, which is consistent with the results of XRD.

Table 2 The analytical result of DSC and DMA

	Transition temperatures and enthalpies in DSC			The storage and loss modulus(Tg+50°C); dissipation factor and glass transition temperature in DMA			
	T_{gsoft} (°C)	T_m (°C)	△H (J/g)	$T_{g\ soft}$(°C)	$T_{g\ hard}$ (°C)	E′(MP)	E″(MP)
HPU	4.2	141.9	6.4	31.4	156.6	6.4	1.2
FPU	7.5	124.1	4.0	38.2	139.8	3.8	1.0

DSC **analysis**

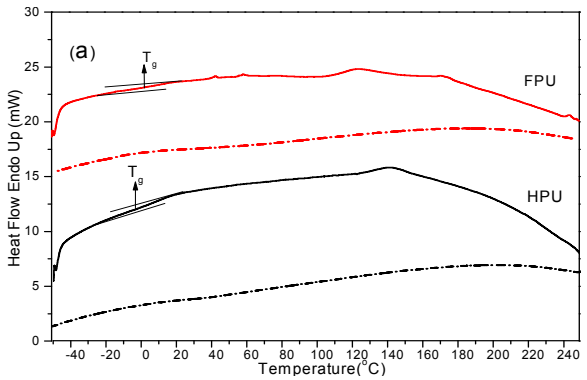

Dynamic mechanical analysis

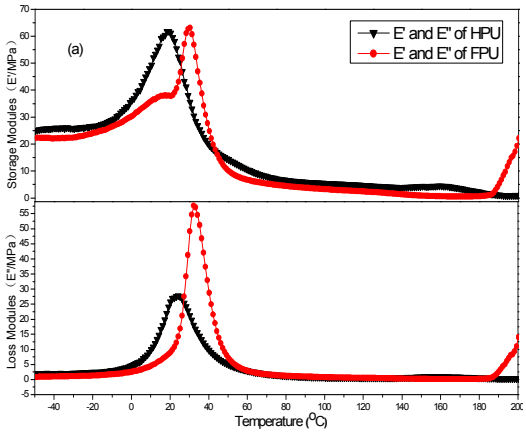

View Article Online
DOI: 10.1039/C5NJ01772F
Journal Name

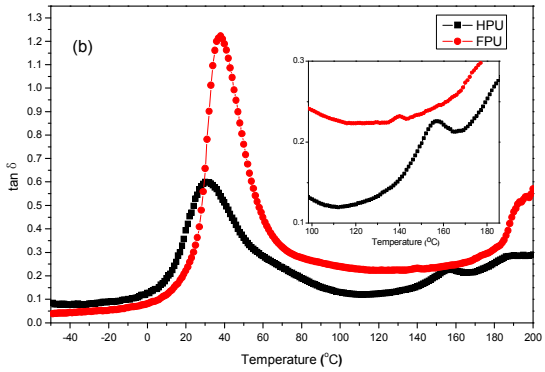

Fig.7 DMA analysis comparison between HPU and FPU: (a)the modulus vs temperature (b) tan δ vs temperature

Dynamic mechanical analysis provides information on glass transition and the mechanical behavior of a polymer. The dynamic mechanical properties of HPU and FPU are shown in Fig. 7. From the modulus vs temperature curves (Fig. 7(a)), the storage modulus and loss modulus in theglassy plateau region of HPU are higher than that of FPU. In order to better understand the effect of fluorinated side chain on the phase separation, the rubber plateau modulus (at temperature T_g+50 °C) is listed on Table 2. It can be observed that an increased rubber plateau storage modulus for HPU but a decreased rubber plateau storage modulus for FPU. The increase in storage modulus of HPU is believed to be the formation of more continuous hard phase morphology. The decreased storage modulus of FPU indicates enhanced phase mixing as introducing fluorinated side chain into polyurethane.[38,39]

On the other hand, polyurethane has two phases. The glass transition temperatures (soft segment and hard segment) of these two phases are very important characteristics of the interaction between soft segment and hard segment. Different from the results of DSC, all the samples exhibited two loss peaks corresponding to the glass transition temperatures of soft segment and hard segment (Fig 7 (b)). The T_g obtained from DMA for HPU and FPU are somewhat higher than the DSC T_g, as expected from the dynamic nature of DMA experiments.In comparison with the loss peaks of HPU, the loss peak of FPU corresponding to soft segment is shifted toward higher temperature, the loss peak of hard segment is shifted toward lower temperature, resulting in the increase in T_g of soft segment and decrease in T_g of hard segment. The result can be considered that the introduction of F into soft segment enhances interactions between soft and hard segments, leading to the reduction of the extent of microphase separation. In addition, the constraint given by the hard phase reduced the degree of freedom of the soft chains. Thereby the onset of large-scale motion of a polymer near T_g requires a higher energy, increasing the value of tan δ peak.[35,40]

Table3 Thermal stability of HPU and FPU

sample	Weight remained (%)[a]			Temperature (°C)[b]			
	300°C	400°C	500°C	T_{10}	T_{50}	$T_{hard\ max}$	$T_{soft\ max}$
HPU	94.7	24.9	4.7	317	362	350	400
FPU	97.9	48.3	9.7	340	398	378	427

[a] Weight losses of HPU and FPU at 300°C , 400 °C, and 500 °C.
[b] 10% and 50% weight temperature, and the maximum degradation temperature.

Mechanical properties analysis

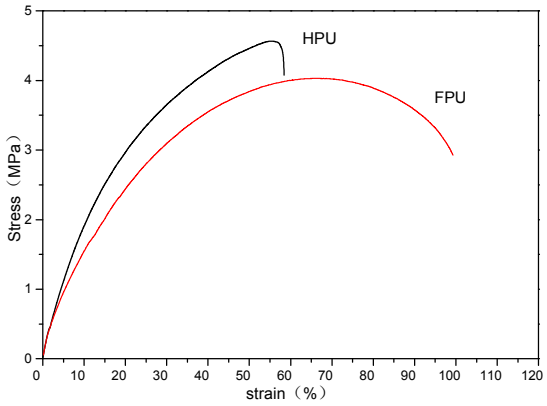

Fig. 8 Strain-stress curves of HPU and FPU

The changed degree of phase separation or mixing can be also reflected from tensile properties, since the tensile strength is remarkably affected by two-phase structure of polyurethanes. Fig.8 showed the stress-strain curves of HPU and FPU. It can be found that a decreased ultimate tensile strength and modulus (the slope), but an increased elongation at break after introducing fluorinated side chain on the soft segment. The decrease in tensile strength should be due to the lower crystalline order, which is consistent with the results of DSC. And also, from above DMA results, the increased tensile strengths in HPU can be understood as due to the increased phase separation, and the decreased tensile strengths in FPU is due to the increased phase mixing. [41]

Thermal stability analysis

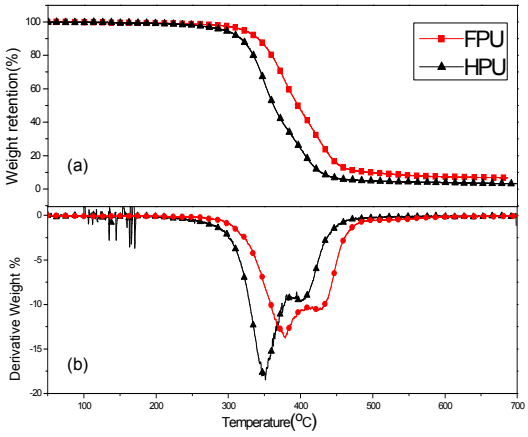

Fig. 9 TGA analysis comparison between PU and FPU: (a) TGA and (b)DTG curves

The thermal degradation of polyurethane is characterized by the decomposition of urethane bonds, the degradation of soft segments, and the evolution of the volatile components.[42]Fig.9 displays the TGA and DTG curves of FPU and HPU. Obviously, the DTG curves

Journal Name

View Article Online
DOI: 10.1039/C5NJ03172F

exhibit two degradation stages. The first degradation stage appearing in the temperature from 300 to 400 °C can be attributed to the decomposition of urethane bonds. The second degradation stage associated with the dissociation of the soft segments occurs from 400 to 500 °C.[43, 44] And also, the characteristic thermal decomposition temperature of HPU and FPUs are shown in Table 3. All the T_{10}, T_{50}, $T_{hard\ max}$ and $T_{soft\ max}$ of FPU are higher than those of HPU and reach 340, 398, 378 and 427°C, respectively. Meanwhile, the char yield of FPU (6.23 %) is higher than that of HPU (2.43 %). It can be concluded that FPU has a better thermal stability than HPU, although FPU and HPU have the same type of hard segments and chain extender.

Corrosion resistance of FPU and HPU

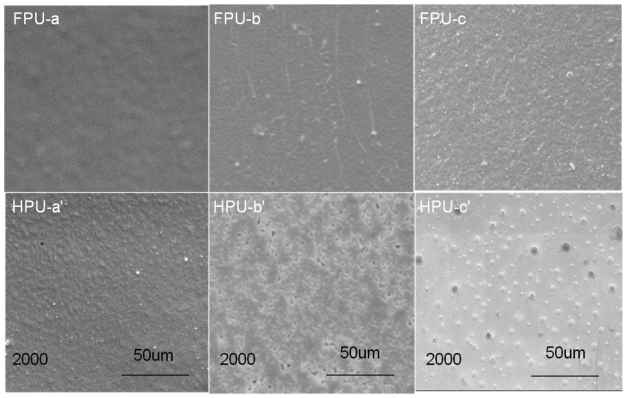

Fig.10 SEM for HPU and FPU corroded by immersion in 40 wt% NaOH and for H_2SO_4 24 h at room temperature: (FPU-a),original FPU sample; (HPU-a') original HPU sample; (FPU-b) and (HPU-b'), FPUs and HPU corroded in 40 wt% NaOH for 24h, respectively; (FPU-c)and (HPU-c'), FPUs and HPU corroded in 40 wt% $H_2SO_4$for 24h, respectively.

Corrosion resistances of FPU and HPU films were evaluated by immersing samples in 40 wt% aqueous solution of NaOH and H_2SO_4 shown to mimic the high corrosive environment. After immersion in 40 wt% aqueous solution of NaOH and H_2SO_4at room temperature for 24 h. The original surface of HPU film under SEM shows grooves, whereas almost no grooves are observed on FPU films (Fig. 10(FPU-a, HPU-a')), suggesting that the introduction of F into HPU soft segments strengthens the interactions between soft and hard segments, thus reducing the degree of microphase separation. A comparison between HPU and FPU exposed to 40 wt% NaOH and H_2SO_4 is show in Fig.10(FPU-b, c HPU-b',c'), it can be seen that HPU shows signs of deep, aggressive corrosion after immersion in 40 wt% NaOH and H_2SO_4, but FPU is devoid of significant surface corrosion. These analyses confirm that the introduction of fluorine enhances corrosion resistance of polyurethane film.

Surface properties of FPU and HPU

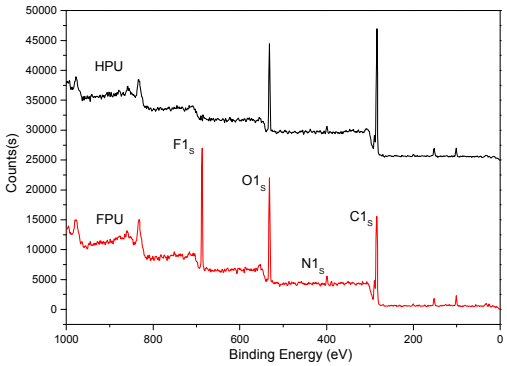

Fig.11 The XPS survey spectra of HPU and FPU

Fig. 12 Shape of water drop on HPU(a) and FPU(b)

Table 4 Contact angle and surface energy of HPU and FPU

Sample	F% in bulk (mol%)	F% in surfac （mol%）	Contact angle (°)	Surfaceenergy (mN/m)
HPU	0	0	78.3	36.18
FPU	12.18	14.48	104.1	21.02

The surface properties of FPU and HPU were studied by XPS and contact angles. To study the surface compositions and the structure of HPU and FPU, the XPS analysis has been carried out. The XPS spectra of HPU and FPU were shown in Fig.11. Compared with HPU, the photoionization peaks of carbon, oxygen, nitrogen and fluorine were observed in the FPU survey spectra. The bulk fluorine molar percent and surface fluorine molar percent were listed in Table 4. It can be found that the surface fluorine contents were higher than the bulk fluorine, due to the migration and enrichment of fluorinated group. In addition, the results of contact angles and surface energy of HPU and FPU with water drop listed in Table 4 showed that FPU had significantly higher contact angle and lower surface energy than that of HPU. This clearly indicates that the FPU exhibit hydrophobic and unique low surface energy as a result of introducing the fluorinated groups into soft segment, and also the surface tension was decreased. The variance of contact angles of FPU and HPU with water drop can be clearly seen from Fig.12.

View Article Online
DOI: 10.1039/C5NJ01772F
Journal Name

The analysis of the curing kinetics of HPU and FPU

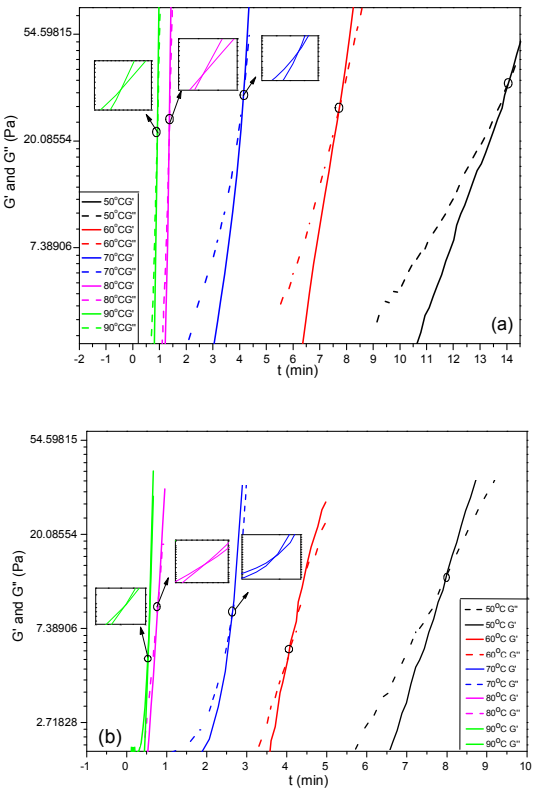

Fig.13 Solidification point measurement of HPU(a)and FPU(b)

Table 5 The t_s and conversion at $t_s$of FPU andHPU

Temperature	HPU		FPU	
(°C)	t_s(min)	α_{t_s}(%)	t_s(min)	α_{t_s}(%)
50	14.07	35.8	8.08	47.9
60	7.76	36.9	4.05	48.1
70	4.14	34.8	2.46	48.7
80	1.35	36.9	0.77	49.0
90	0.92	35.7	0.51	48.6

The curing reaction of HPU and FPU was studied through solidification point measurements at various temperatures, as shown in Fig. 13.The crossovers points of G' and G" are defined as the solidification point (t_s) [45,46]. t_s of FPU and HPU is the temperature in which FPU and HPU have no fluid properties. It can be seen that the t_s decrease with the rise of temperature, it might be attributed that the increase of temperature speeds up the reaction rate, leading to a faster consumption of NCO. A comparison between the t_s of HPU and FPU at the same temperature is listed in Table.5. It can be seen that the reaction process is directly related to the initial monomer structure. When using fluorinated polyether as soft segment, the t_s is slightly shorter. These phenomena are concerned in the reactivity of the hydroxyl in polyether. The higher electronegativity of fluorine in FPO strongly influences the charge distribution of the hydroxyl, and corresponding, increases the reactivity of the hydroxyl, leading to the increase of the rate of curing reaction and reduction in the t_s apparently. The reaction mechanism of urethane formation is as flow:

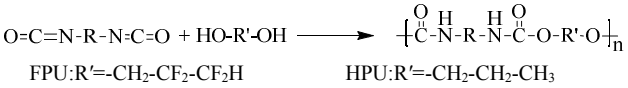

Absorbance FTIR spectra was registered to measure the conversion of the NCO at t_s. The ratio between the absorbances at 2270 cm^{-1} and the reference (constant) band at 1530 cm^{-1} was considered in order to evaluate the conversion of NCO content at t_s. Because the absorbance at 1530 cm^{-1} was the stretching vibrations of the benzene ring, did not overlap with other peaks and thus provided a direct means of monitoring the NCO concentration. The conversion of the NCO at t_s obtained from the FTIR spectra (a_{IR}) was calculated according to the following equation [47]:

$$\alpha_{IR} = 1 - \frac{I_{NCO.G} I_{R.O}}{I_{NCO.O} I_{R.G}}$$

Where $I_{NCO.O}$ and $I_{R.O}$ are the initial peak intensities of the NCO and reference bands, respectively, and $I_{NCO.G}$ and $I_{R.G}$ are the peak intensities of the same bands at t_s. We experimented at least six times and took the average. The results are listed at Table 5. It can be seen that the conversions of HPU and FPU at t_s are almost constant. The average value of the FPU conversion at the t_s is 48.46%. The value of FPU is slightly higher than the HPU value of 36.02%, and the difference is due to the higher rate of curing reaction of FPU.

Under the kinetically controlled conditions, the reaction rate can be expressed by an Arrhenius rate expression as follows[48-50]:

$$\frac{da}{dt} = A \exp(-\frac{E}{RT}) f(a) \quad (1)$$

Where a is the conversion, A is a constant factor, E is the activation energy, T is the curing temperature, and $f(a)$ is the conversion-dependent function, independent of the curing temperature. By integrating from a=0 to a=a_{t_s}, the equation becomes

$$\ln t = \frac{E}{RT} + \left[\ln\left(\int_0^{a_{ts}} \frac{da}{f(a)}\right) - \ln A\right] \quad (2)$$

Since the terms in the last part of right side of equation are constant for a fixed conversion, the equation becomes

$$\ln t = C + \frac{E}{RT} \quad (3)$$

Fig. 14 shows the Arrhenius plot of ln $t_s$versus 1/T for HPU and FPU. The apparent activation energy Ecan be calculatedfrom the slope The activation energy E and the constant C can be determined from the slope and the intercept of the linear relationship between ln t vs. 1/T. The results were listed in table 6. It can be found that linear correlations coefficient were up to 0.988 and 0.955 ,which indicates the validity of this method. We obtained the activation energy of HPU is 75.51 kJ·mol^{-1}. And the activation energy of FPU is 70.24kJ·mol^{-1}, lower than the values of HPU, indicating that the curing reaction of FPU is much easier than that of HPU, which is in accordance with the analysis of the t_s.

Journal Name

View Article Online
DOI: 10.1039/C5NJ01772F ARTICLE

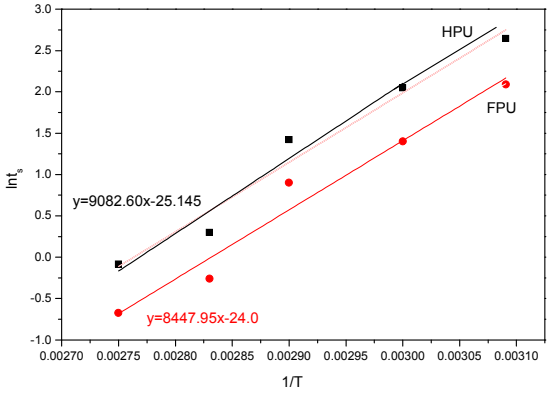

Fig.14 Plots of $\ln t_s$ versus 1/T of HPU and FPU

Table 6 Activation energy of FPU and HPU

Saple	The linear correlation coefficient	the slope of the lines	conversion C	*E*a (kJ/mol)
FPU	0.988	8447.95	-25.15	70.24
HPU	0.956	9082.60	-24.0	75.51

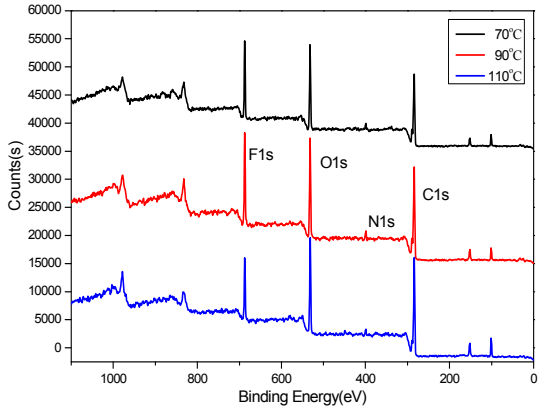

Fig.15 XPS survey spectra of FPU

To sutdy the influence of curing process on the mobility of fluorinated groups to the surface ofFPU, the XPS analysis of FPU was carried out.The XPS survey spectra is shown in Fig. 15. The XPS measurements showed the photoionization peaks of carbon, oxygen, nitrogen and fluorine in the FPU survey spectra. The peak intensity of F1s in the surface is higher at low temperature than that at high temperature. In addition, the peak intensity of N1s was weak due to the lower content of hydrophilic urethane groups in the surface layer. The surface element molar percents obtained by XPS were list in Table 7. It can be seen that the amount of surface fluorine increases with decreasing thecuring temperature, indicating thatthe curing process has a great influence on the mobility of fluorinated groups .From the result of the analysis of t_s, we knew that with increasing temperature, the $t_s$decreases and the curing rateincreases. Thus, there is not enough time for fluorinated groupsto migrate to the surface of FPU, leading to the decrease of F content in FPU surface.Thus it can be concluded that to select the appropriate curing temperature is propitious for the movement of fluorinated group and flurorinesurface enrichment.

Table 7 Element percentage onS-FPU surface

Temperature (℃)	suface element molar percent (mol%)			
	C	O	N	F
70	46.81	34.23	4.48	14.48
90	52.24	34.19	3.96	9.61
110	52.44	37.41	3.56	6.59

Conclusions

A novel fluorinated polyurethane (FPU) featuring fluorine-containing side chains was successfully synthesized by fluorinated polyether glycol with fluorine-containing side chains as soft segments, MDI as hard segments and 1,4-butanldiol (BDO) as chain extenders. The structure of the FPU was characterized by FTIR and NMR. SEM directly reveals that the extent of microphase separation reduces as the introduction of fluorinate into the soft segment. Moreover, the reduction of the microphase separation between the soft and hard segments decreases the crystallinity of FPU, and increases the T_g of soft segments and decreases the T_g of hard segment. Meanwhile the thermal stability, surface property and corrosion resistance of FPU have been significantly enhanced. Furthermore, the results of the curing kinetics showed that the introduction of F into polyurethane increased the curing rate, and E_a of FPU (70.24 kJ·mol^{-1}) is lower than that of HPU (75.51 kJ·mol^{-1}). XPS analytical result showed that there was an obvious effect of the curing process on the mobility of fluorinated groups to the surface of FPU.

Acknowledgements

This project was supported by Natural Science Foundation of China (NO.3212310008), the innovation project of the shanghai Municipal Education Commission(No.15ZZ076) and the Hujiang Foundation of China(B14006).

Notes and references

[a]*School of Materials Science and Engineering, East China University of Science and Technology, Shanghai 200237, China.*

[b] *School of Materials Science and Engineering, University of Shanghai for Science and Technology, Shanghai 200093, China.*

[c]*Department ofPolymer Chemistry and Physics, Shanghai Normal University, Shanghai 200234, China.*

E-mail address: qzhdong@ecust.edu.cn;liying@usst.edu.cn;

Fax: +86-21-64251123. Phone: +86-21-64251123

1 D. K. Chattopadhyay, K. V. S. N. Raju. *Prog. Polym. Sci*., 2007, **32**, 352.
2 X. L. Li, Z, Fang, X. Li, S. G. Tang. K. Zhang. *New J. Chem*., 2014, **38**, 3874.
3 Z. Y. Lan， R. Daga, R. Whitehouse, S. McCarthy, D, Schmidt. *Polymer*. 2014, **55**, 2635.
4 W. J. Lee, M, S, Lin. *J. Appl. Polym. Sci*., 2008, **109**, 23.
5 M. Y. L Chew, X. Zhou, Y, M, Tay. *Poly. Test*., 2001, **28**, 87.
6 P. Krol. *Prog. Mater. Sci*., 2007, **52**, 915.
7 C. B. McCloskey, C. M. Yip, J. P. Santerre. *Macromolecules*, 2002, **35**, 924.
8.Z. Ge, X. Y. Zheng, J. B. Dai, W. H. Li, Y. J. Luo. *Eur. Polym. J*., 2009, **45**, 530.
9 C. Wang, X. R. Li, B. Du, P.Z. Li. *Colloid. Polym Sci*., 2014, **292**, 579.
10 M. Zhang, S.L.Zhou, J.*Univ. Shanghai. Sci. Technol*.,1998,**3**,272.
11 S. Turri,M. Levi,T. Trombetta,*J. Appl. Polym. Sci*.,2004,**93**, 136.
12 S, Turri, M. Levi, T. P. Trombetta,*Macromol. Symp*.,2004,218, 29.

View Article Online
DOI: 10.1039/C5NJ01772F Journal Name

13 Y. S. Kim, J. S. Lee,Q. Ji,J. E. McGrath,*Polymer*,2002,**43**, 7161.
14 V. Durrieu,A.Gandini, *Polym. Adv. Tech.*, 2005,**16**, 840.
15 M. J. Zhu,F. L. Qing,W. D. Meng,*J. Appl. Polym. Sci.,*2008,**109**, 1911.
16 C. H. Lim, H. S.Choi, S. T. Noh.*J. Appl. Polym. Sci.,* 2002, **86**, 3322.
17 Z. Ge, X. Y. Zhang, J. N. Dai. *J.Macromol. Sci. PartA: Pure Appl. Chem.*,2009, **46**, 215.
18 C.Tonelli, G. J. Ajroldi, *J. Appl. Polym. Sci.,*2003, **87**, 2279.
19 S. C. Yoon, B. D. Ratner. *Macromolecules*, 1988, **21**, 2392.
20 S. C. Yoon, B. D. Ratner. *Macromolecules*, 1988, **21**, 2401.
21 P. F Liu, L. Ye, Y. G. Liu, F. D. Nie. *Polym. Bull*., 2011, **66**, 503.
22 M. Castellano, C.Tonelli, A. Turturro. *J Mater Sci.,*2014, **49**, 2519.
23 T. Liu, L. Ye, *J. Fluorine Chem*., 2010, 131, 36.
24 R. P. Jia, A, X, Zong, X. Y. He, J. Y. Xu, M. S. Huang, Fiber. Polym., 2015, **16**, 231**.**
25 G. Marchionni, G, Ajroldi, M. C. Righetti, G. Pezzin. Macromolecules, 1993, **27**, 1751.
26 A. Milani, J. Zanetti, C. Castiglioni, E. D. Dedda, S. Radice. *Eur. Poly. J*, 2012, **48**, 391.
27 L. Mashlyakovskiy, V. Zaiviy, G. Simeone, C. Tonelli,*J. Polym. Sci.: Part A: Polym. Chem.,*1999, **37**, 557.
28 S. Turri, T. Trombetta, M. Levi,*Macromol. Mater. Eng.* 2000, **283**, *144.*
29 L. L. Li, Y. Li, X. Wang, Q. Z. Dong, *Emerg. Mater. Res*., 2015, **4**, 102.
30 L. L. Li, Y. Li, X. Wang, Y. C. Qing, J. J. Hu, *J. Fluorine Chem*.,2015, **175**, 129.
31R.M.Romano, J.Czarnowski, C. O. D.Vedova,*Inorg.Chem.,* 2001, **40**, 3039.
32 M. E.Ryan,J. L. C. Fonseca, S.Tasker,J. P. S. Badyal,*J. Phys. Chem.,*1995, **99**, 7060.
33Y. J.Xu,Z.Petrovic, S.Das,G. L.Wilkes, *Polymer*,2008, **49**, 4248.
34 L. F.Wang, *Polymer*, 2007, **48**, 894.
35 W. W. Yu, M.Du, D. Z.Zhang,L.Yu, Q.Zheng, *Macromolecules*,2013, **46**, 7341.
36 A. M. Castagna, A. Pangon，T. Choi，G. P. Dillon,*Macromolecules*, 2012, **45**, 8438.
37 C. Tonelli, G. Ajroldi, A. Turturro, A. Marigo, Polymer, 2001, **42**, 5589.
38 H. Tan, J. H. Li, R. G. Du. Polymer, 2005, **46**, 7230.
39 Y. J. Xu, Z. Petrovic, S. Das, G. L. Wilkes, Polymer, 2008, 49, 4248.
40 C. B. Wang, S. L. Cooper.*Macromolecules*, 1983,**16**,775.
41 P. F. Liu. L. Ye. Y. G. Liu, F. D. Nie, *Polym. Bull.,*2011, **66**, 503.
42 Y. J. Xu, Z. Petrovic, S. Das, *Polymer*,2008,**49**,4248.
43 M. G. Lu, J. Y.Lee, M. J.Shim, S. W.Kim, *J. Appl. Polym. Sci.*, 2002, **85**, 2552.
44 H. Q. Fu, C. B. Yan, W. Zhou, H. Huang,*Comp. Sci. Tech.*,2013, **85**, 65.
45 Xu Weibing, He Pingsheng, Chen Dazhu. *Eur. Polym. J.*, 2003,39, 617..
46 Tung, C. Y. M., Dynes, P. J., *J. Appl. Polym. Sci.*,1982, 27, 569-574.
48 D. Olmos, A. Loayza, J. González-Bentito. *J. Appl. Polym. Sci.*, 2010, 117, 2695.
49 R. Rodriguez, B. Perez, J. Adhes., 2014, **90**, 848.
50 L. Nu´n˜ez, J. Taboada, F. Fraga, M.R. Nu´n˜ez, *J. Appl. Polym. Sci.*, 1997, **66**, 1377.
51 S. Cho, E. P. Douglas, J. Y. Lee, *Polym. Eng. Sci*., 2006, **46**, 623.
.

View Article Online
DOI: 10.1039/C5NJ01772F

For the Table of Contents Entry

The synthesis and curing kinetics study of a new fluorinated polyurethane with fluorinated side chains attached to soft blocks

Lingling Li, Xia Wang*, Zan Li , Ying Li* , Yuanchun Qi , Qingzhi Dong*

Fluorinated polyurethane with fluorinated side chains attached to soft blocks was successfully synthesized, which exhibited unique properties. And also the curing kinetics was studied using rotational rheometer.